

## Hydrodynamics, sediment transport, and morphodynamics in the Vietnamese Mekong Delta: Field study and numerical modelling

Doan Van Binh<sup>a,b,\*</sup>, Sameh A. Kantoush<sup>b</sup>, Riadh Ata<sup>c</sup>, Pablo Tassi<sup>d</sup>, Tam V. Nguyen<sup>e</sup>,  
Jérémy Lepesqueur<sup>f,g</sup>, Kamal El Kadi Abderrezzak<sup>d</sup>, Sébastien E. Bourban<sup>d</sup>,  
Quoc Hung Nguyen<sup>a</sup>, Doan Nguyen Luyen Phuong<sup>a</sup>, La Vinh Trung<sup>h</sup>, Dang An Tran<sup>i</sup>,  
Thanh Letrung<sup>i</sup>, Tetsuya Sumi<sup>b</sup>

<sup>a</sup> Faculty of Engineering, Vietnamese-German University, Binh Duong Province, Viet Nam

<sup>b</sup> Water Resources Research Center, Disaster Prevention Research Institute, Kyoto University, Goka-sho, Uji City, Kyoto, Japan

<sup>c</sup> Flow Science, Santa Fe, NM, USA

<sup>d</sup> National Laboratory for Hydraulics and Environment, Research & Development Division, Electricité de France and Saint-Venant Hydraulics Laboratory, Chatou, France

<sup>e</sup> Department of Hydrogeology, Helmholtz Centre for Environmental Research, Leipzig, Germany

<sup>f</sup> Environmental Research and Innovation Department, Luxembourg Institute of Science and Technology, Belvaux, Luxembourg

<sup>g</sup> Météo-France DIRAG/EC-MPF, DESAIX, BP Fort-de-France, France

<sup>h</sup> Research Management Department, Vietnamese-German University, Binh Duong Province, Viet Nam

<sup>i</sup> Thuyloi University, Dong Da, Hanoi, Viet Nam

### ARTICLE INFO

#### Keywords:

Morphological change  
Diversion channel  
Riverbed incision  
Scour hole  
Sediment reduction  
2D numerical modelling

### ABSTRACT

Flow, suspended sediment transport and associated morphological changes in the Vietnamese Mekong Delta (VMD) are studied using field survey data and a two-dimensional (2D) depth-averaged hydromorphodynamic numerical model. The results show that approximately 61–81 % of the suspended sediment load in the Hau River during the flood seasons is diverted from the Tien River by a water and suspended sediment diversion channel. Tidal effects on flow and suspended sediment load are more pronounced in the Hau River than in the Tien River. The results show the formation of nine scour holes in the Tien River and seven scour holes in the Hau River from 2014 to 2017. Additional six scour holes are likely to form by the end of 2026 if the suspended sediment supply is reduced by 85 % due to damming. Notably, the scour holes are likely to form at locations of severe riverbank erosion. In the entire study area, the simulated total net incision volume in 2014–2017 is approximately 196 Mm<sup>3</sup> (equivalent to 65.3 Mm<sup>3</sup>/yr). The predicted total net incision volumes from 2017 to 2026 are approximately 2472 and 3316 Mm<sup>3</sup> under the 18 % and 85 % suspended sediment reduction scenarios, respectively, thereby likely threatening the delta sustainability. The methodology developed in this study is helpful in providing researchers and decision-makers with one way to predict numerically the scour hole formation and its association with riverbank stability in river deltas. Of equal importance, this research serves as a useful reference on the role of water and suspended sediment diversion channels in balancing landforms in river-delta systems, particularly where artificial diversion channels are planned.

### 1. Introduction

Sediments transported by rivers are the major sources of materials for protecting deltas from the natural processes of subsidence. However, sediment loads worldwide have been significantly reduced by climate change and anthropogenic activities (e.g., damming, mining, urbanization) (Maeda et al., 2008; Lu et al., 2015; Darby et al., 2016; Binh et al.,

2020b; Hackney et al., 2020; Park et al., 2022), causing detrimental impacts on landforms, aquatic environments, and salinity intrusion in river-delta systems (Kondolf et al., 2014a; Best, 2019; Eslami et al., 2019; Binh et al., 2021; Loc et al., 2021). The Vietnamese Mekong Delta (VMD) is not an exception.

The flow regime of the Mekong River, which is one of the largest river systems worldwide and most important food-producing regions in

\* Corresponding author at: Faculty of Engineering, Vietnamese-German University, Binh Duong, Viet Nam.

E-mail address: [binh.dv@vgu.edu.vn](mailto:binh.dv@vgu.edu.vn) (D.V. Binh).

<https://doi.org/10.1016/j.geomorph.2022.108368>

Received 10 January 2022; Received in revised form 30 June 2022; Accepted 2 July 2022

Available online 8 July 2022

0169-555X/© 2022 Elsevier B.V. All rights reserved.

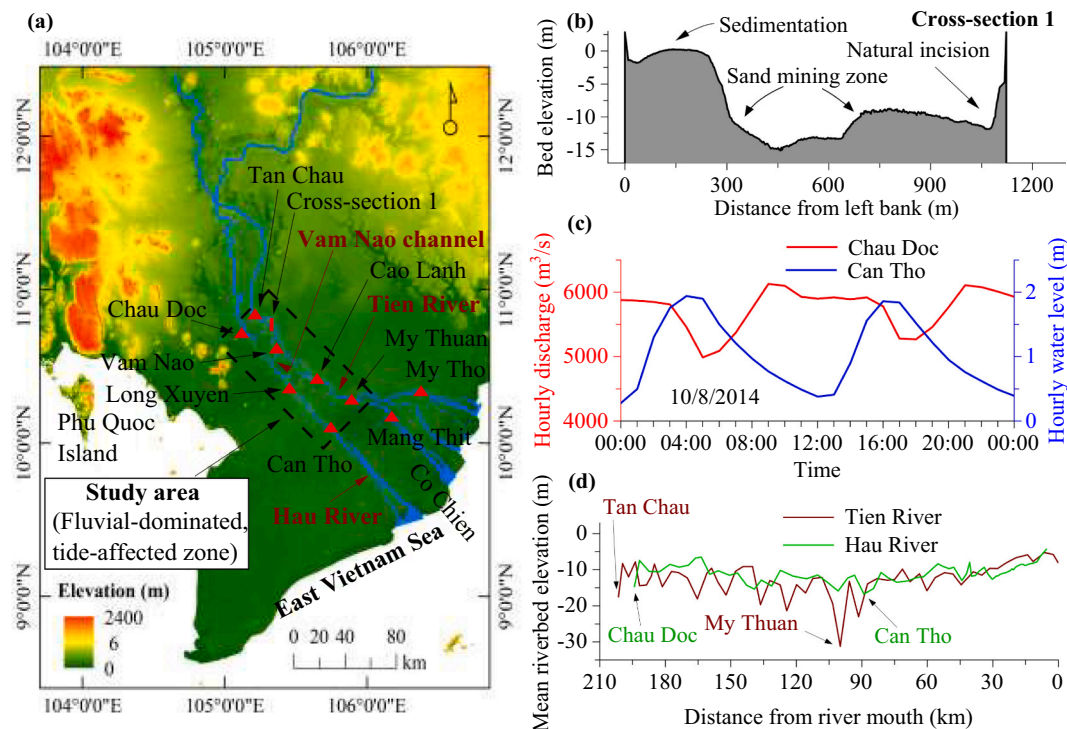


**Fig. 1.** Vietnamese Mekong Delta: (a) major rivers and hydrological stations (red triangle symbols); (b) a typical cross-section where sand mining causes riverbed incision; (c) the hourly flow discharge and water level at Chau Doc and Can Tho during the flood season; and (d) longitudinal riverbed profiles along the Tien and Hau Rivers. The digital elevation map shown in panel (a) is from the Shuttle Radar Topography Mission (SRTM) with a 30-m spatial resolution downloaded from <https://dwtkns.com/srtm30m/>. Among the eight gauging stations indicated in panel (a), Tan Chau, Chau Doc, Vam Nao, My Thuan, and Can Tho monitor water level, discharge, and SSC; Long Xuyen, Cao Lanh, and My Tho monitor water level.

Southeast Asia (Boretti, 2020), has been significantly altered (Lauri et al., 2012; Lu et al., 2014; Binh et al., 2018; Hecht et al., 2019; Binh et al., 2020a, 2020c), with the suspended sediment load (SSL) being substantially reduced (Kummu and Varis, 2007; Kondolf et al., 2014b; Binh et al., 2020b). Six mainstream dams in the Lancang cascade (upper Mekong basin) have reduced the SSL by 50–94 % along the lower Mekong River (Kummu et al., 2010; Kondolf et al., 2014b; Manh et al., 2015), and sixty-four completed dams in the Mekong basin were responsible for a 74 % SSL reduction in the VMD (Binh et al., 2020b). Additionally, sand mining activities have accelerated in the VMD, jumping from 7.75 Mm<sup>3</sup>/yr in 2012 (Bravard et al., 2013) to 29.3 Mm<sup>3</sup>/yr in 2018 (Jordan et al., 2019); these values are likely underestimated compared to an average volume of 42 Mm<sup>3</sup>/yr during 2015–2020 (Gruel et al., 2022) considering illegal mining activities. Overall, damming and sand mining have caused severe morphological degradation and salinity intrusion in the VMD (Anthony et al., 2015; Li et al., 2017; Mai et al., 2018, 2019a, 2019b; Eslami et al., 2019; Jordan et al., 2019; Binh et al., 2020d).

Flow, suspended sediment transport, and morphodynamic processes in the VMD are not fully understood due to the hydrological and hydraulic complexity of the system (i.e., seasonal interactions between fluvial flows and tidal currents) and scarcity of field data. While the delta covers an area of 39,000 km<sup>2</sup>, there are only five gauging stations that monitor flow and suspended sediments. Some studies analysed the flow and SSL at these stations (e.g., Dang et al., 2016; Ha et al., 2018; Binh et al., 2020a, 2020b, 2021), while other studies dealt with suspended sediment dynamics in some floodplain and coastal areas only (e.g., Wolanski et al., 1996; Hung et al., 2014a, 2014b). Large parts of the VMD is mostly unknown and its morphodynamics remains unexplored because the bathymetry has not been monitored regularly.

Scour holes in tidal channels are formed at confluences (Rice et al., 2008), outer banks of meandering channels or sand mining locations (Jordan et al., 2019; Hackney et al., 2020), under complex

hydrosedimentary processes caused by the alternating flood/ebb of tidal currents (Ferrarin et al., 2018). Bedload is trapped in scour holes (Anh et al., 2022), which induces progressive (regressive) erosion far downstream (upstream). Scour hole formation and evolution in the VMD are unexplored. Moreover, quantifying water and suspended sediment interchange between the two main rivers (Tien and Hau Rivers) via the Vam Nao diversion channel has not been adequately assessed at the monthly or seasonal scales.

To overcome the scarcity of measurements, remotely sensed satellite data have been employed (Loisel et al., 2014; Dang et al., 2018) and numerical models have been applied to simulate hydrodynamics (Wassmann et al., 2004; Van et al., 2012) and suspended sediment dynamics (Xue et al., 2012; Hein et al., 2013; Manh et al., 2014, 2015; Vinh et al., 2016; Thanh et al., 2017; Xing et al., 2017; Tu et al., 2019; Le, 2020). Xing et al. (2017) found numerically that sand is exported from and imported into the lower Hau River in the high-flow and low-flow seasons, respectively. According to Tu et al. (2019), erosion and deposition occurred alternately along the coast, whereas the preliminary results by Thuy et al. (2019) showed that erosion is more dominant and severe in the upper part (upstream of My Thuan) of the Tien River, but is relatively low in the estuaries. Jordan et al. (2020) found that hydro-power dams have the strongest impact on riverbed incision, amplified by sand mining, whereas relative sea level rise has the lowest effect. Recently, Anh et al. (2022) estimated, for the first time, the effect of sand mining and dredging on morphological dynamics in the Soai Rap River using the Telemac modelling suite of codes. Although the model, which was neither calibrated nor validated, encompassed the lower VMD main rivers, Anh et al. (2022) focused only on the Sai Gon–Dong Nai River system. Overall, the existing studies have focused either on the lower part of the VMD and coastal zone (Xing et al., 2017; Tu et al., 2019) or on a small region in the upper VMD (Jordan et al., 2020), while the suspended sediment transport and morphodynamics in the whole upper VMD have been largely ignored. The studies did not provide sufficient

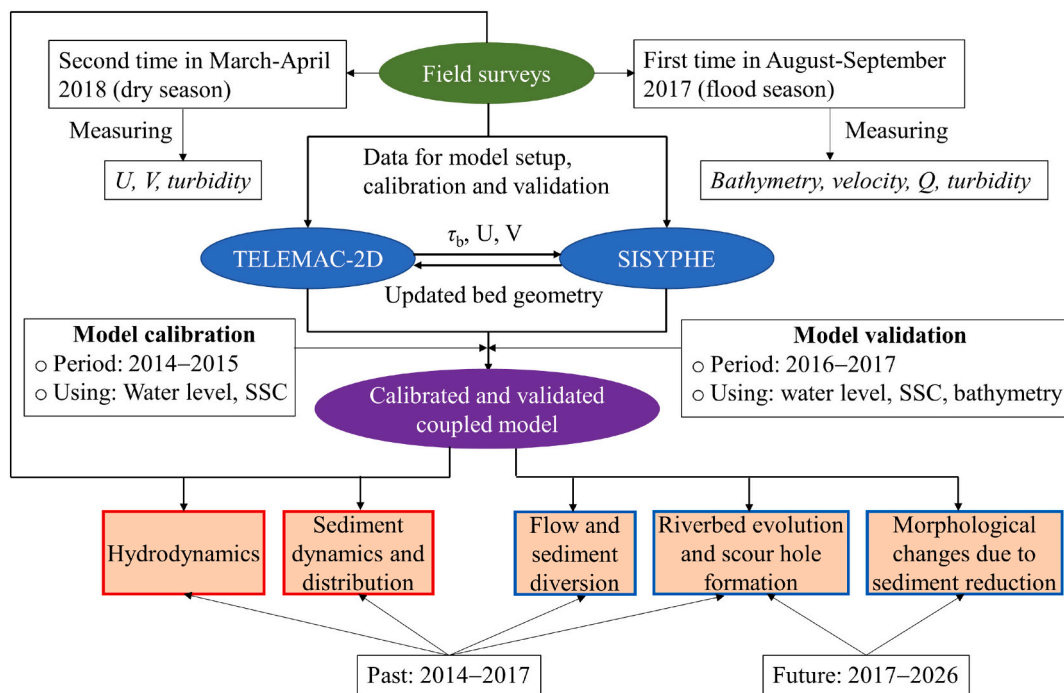


Fig. 2. Methodological framework adopted in this study.  $U$ ,  $V$ : velocities in the  $x$ - and  $y$ -direction.  $\tau_b$ : critical bed shear stress.  $Q$ : discharge.

understanding of either the inter- or intra-annual variations in the morphodynamics in the VMD or the formation of scour holes that cause riverbank instability (Hackney et al., 2020). Although authorities and researchers know well about the hydrological role of the Vam Nao diversion channel, but quantitative estimates of inter-intra-sediment diversion remain unknown.

Using field data and numerical modelling, this study aims therefore at addressing quantitatively the formation of scour holes in the VMD, and the role of the diversion channel in diverting suspended sediment between the river systems is comprehensively evaluated. The present work provides a crucial reference for other deltas where the construction of artificial diversion structures may be planned or constructed (e.g., in Mississippi and Yellow River deltas) (Guan et al., 2019; Pahl et al., 2020). Moreover, this research is among the pioneering works applying the *open-source* Telemac package ([www.opentelemac.org](http://www.opentelemac.org)) for modelling flow, suspended sediment transport and morphodynamics in the VMD rather than using commercial numerical codes.

The paper is organized as follows: Section 2 describes the study area. Section 3 presents the methodology, including the field measurements, numerical model set-up and simulated scenarios. Results and discussions are given in Section 4, followed by conclusion in Section 5.

## 2. Study area

The VMD is located in the estuary of the Mekong River (Fig. 1a), which discharges approximately 300–550 km<sup>3</sup>/yr of water (Milliman and Farnsworth, 2011; Darby et al., 2016) and 40–167 Mt/yr of suspended sediment (Kondolf et al., 2014b; Nowacki et al., 2015; Binh et al., 2020b) into the East Vietnam Sea via two main distributaries, namely, the Tien and Hau Rivers. Upstream of the Vam Nao diversion channel (Fig. 1a), the Tien River transports approximately 80 % of the flow and suspended sediment from the Mekong River. Due to redistribution of the flow and suspended sediment by the Vam Nao diversion channel, the Tien and Hau Rivers transport similar amounts of water downstream of the diversion channel.

The flow regime in the VMD is characterized by strong seasonality, with two distinct seasons driven by a monsoonal climate: flood season (July–December) and dry season (January–June). The SSL of the VMD

has been reduced by 74 % due to the sixty-four existing dams in the Mekong basin (Binh et al., 2020b), and is expected to decrease by 96 % if all one hundred thirty-three planned dams are completed (Kondolf et al., 2014b). Sand mining increased from 7.75 Mm<sup>3</sup>/yr in 2012 to 29.3 Mm<sup>3</sup>/yr in 2018 (Bravard et al., 2013; Jordan et al., 2019). Fig. 1b shows a typical cross-section where sand mining occurs.

The VMD is located in the fluvial-to-marine transition zone, which is divided into two distinctive zones: the upstream, fluvial-dominated zone and the downstream, tide-dominated zone (Gugliotta et al., 2017). The boundary between these zones is at the My Thuan and Can Tho gauging stations (Fig. 1a). The river areas considered in this study are located in the fluvial-dominated, tide-affected zone (Fig. 1a). During the flood season, tidal influence is limited to the upper VMD (e.g., at Chau Doc) compared to the lower VMD (e.g., at Can Tho) (Fig. 1c) due to high riverine fluvial discharges. However, tide-driven water level fluctuations are significant during the dry season (e.g., approximately 1 m at Tan Chau and Chau Doc and 2 m at My Thuan and Can Tho) (Gugliotta et al., 2017). The flow is bidirectional during the dry season because of the interaction between the semidiurnal tide from the East Vietnam Sea and the riverine discharge from the Mekong River. The rivers are deep and narrow, with bed elevations decreasing seaward (Fig. 1d). The SSL is dominated by silt and clay, accounting for 95 to 98 % of the total load (Koehnken, 2014; Binh et al., 2020b). Bedload, composed of fine sand, constitutes only 1 to 3 % of the total annual load (Gugliotta et al., 2017; Jordan et al., 2019; Hackney et al., 2020).

## 3. Materials and Methods

### 3.1. Methodological framework

Fig. 2 shows a methodological flowchart. We conducted two field surveys along VMD main rivers to measure bathymetry, velocity, discharge and turbidity. These data were combined with the monitored data at gauging stations for analysing flow and suspended sediment dynamics and distribution in the river-delta system. The data were also used to establish a 2D morphodynamic numerical model. The numerical model together with the field data were used to estimate flow and suspended sediment diverted through the Vam Nao diversion channel, to



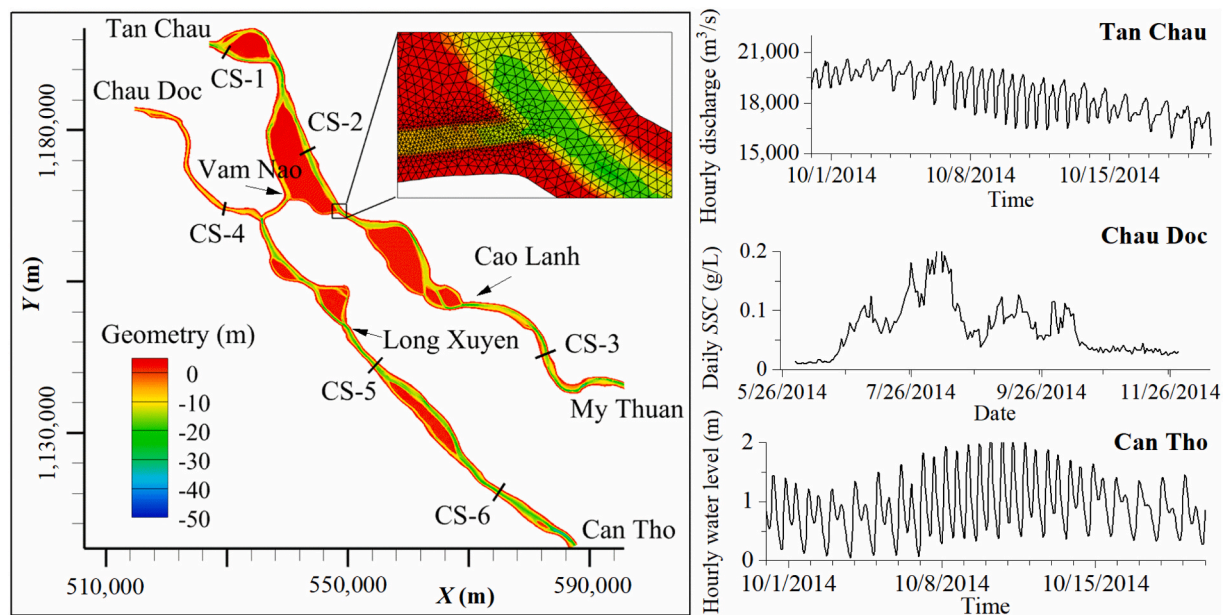


Fig. 3. Geometry and mesh discretization of the computational domain, including locations used for calibrating and validating the model. Representative data of the hourly discharge and daily SSC at upstream boundaries and the hourly water level at downstream boundaries are given.

predict (for the past and future) riverbed evolution and scour hole formation, and to forecast morphological changes under some likely scenarios of reduced suspended load at the upstream end.

### 3.2. Field measurements

Two field surveys were conducted from August to September 2017 (flood season) and from March to April 2018 (dry season) along 570 km of the Tien and Hau Rivers and the Vam Nao channel (Fig. 1a). In the first survey, we measured the river bathymetry (i.e., eighty-two cross-sections), velocity, discharge, and turbidity using an acoustic Doppler current profiler (aDcp) and an Infinity-ATU75W2-USB turbidity meter. Vertical flow velocities were measured every 0.4–1.5 m depending on the water depth. Data processing is given by Binh et al. (2020b). In the second survey, infinity velocity and turbidity meters were used to measure velocity and turbidity longitudinally and vertically. Three to six vertical profiles were recorded at each cross-section depending on the river width. Positions of the profiles were recorded by a handheld Garmin GPS, and the interval of turbidity measurements was 60 s. Turbidity measurements were converted to suspended sediment concentrations (SSCs) using specific equations (see Supplementary Material).

In the first survey, the measured suspended sediment samples at My Thuan and Mang Thit stations in the Tien River (Fig. 1a) yield median diameters  $d_{50}$  of 12.6  $\mu\text{m}$  and 6.1  $\mu\text{m}$ , respectively. The associated settling velocities are 0.052 and 0.012 mm/s, respectively, estimated by Stokes' (1851) law. These values may be underestimated because flocs can be formed for cohesive particles. However, this underestimation does not affect our numerical results because the settling velocity is one of the tuning parameters in the numerical model. Our estimated settling velocity combined with the values published in previous papers (see Section 3.5) serve as a reference for the initial selection of the settling velocity in our model.

### 3.3. Numerical modelling framework

We used the widely known and well-tested Telemac-Mascaret modelling system (Hervouet, 2007, [www.opentelemac.org](http://www.opentelemac.org)) to simulate flow, suspended sediment transport, and morphodynamics in the upper VMD. Hydrodynamics was modelled using the 2D depth-averaged

TELEMAC-2D module, and sediment transport and riverbed evolution were simulated using the SISYPHE module (Villaret et al., 2013; Langendoen et al., 2016). Both the TELEMAC-2D and SISYPHE modules are internally coupled (El Kadi Abderrezak et al., 2016; Sisyph, 2018) and are solved using the finite element method of an unstructured mesh. Telemac-Mascaret can be run in parallel mode, substantially reducing the computational time.

Bedload is negligible in the VMD (Jordan et al., 2019; Hackney et al., 2020). Suspended sediment consists of both cohesive ( $d_{50} < 63 \mu\text{m}$ ) and noncohesive ( $d_{50} > 63 \mu\text{m}$ ) particles (Wolanski et al., 1996; Xing et al., 2017). The suspended sediment transport of the sand-mud mixture is simulated by solving a 2D advection-diffusion equation for the  $k$ th size class ( $k = 1$  for cohesive and  $k = 2$  for noncohesive):

$$\frac{\partial(hC_k)}{\partial t} + \frac{\partial(huC_k)}{\partial x} + \frac{\partial(hvC_k)}{\partial y} = \frac{\partial}{\partial x} \left( h\varepsilon_s \frac{\partial C_k}{\partial x} \right) + \frac{\partial}{\partial y} \left( h\varepsilon_s \frac{\partial C_k}{\partial y} \right) + E^k - D^k \quad (1)$$

where  $t$  is time;  $h$  is the flow depth;  $u$  and  $v$  are depth-averaged flow velocities in the  $x$ - and  $y$ -Cartesian directions, respectively;  $C_k$  is the depth-averaged concentration of the  $k$ th size class (in % volume);  $\varepsilon_s$  is the sediment turbulent diffusivity, usually related to the eddy viscosity by  $\varepsilon_s = \nu_t / \sigma_c$  with  $\sigma_c$  as the Schmidt number (set at 1.0 in SISYPHE); and  $E^k$  and  $D^k$  are erosion and deposition rates of the  $k$ th size class, respectively. SISYPHE computes the bed evolution using the following Exner (1925) equation:

$$(1 - \lambda) \frac{\partial z_b}{\partial t} + (E - D) = 0 \quad (2)$$

in which  $\lambda$  is the bed porosity and  $z_b$  the bed level (m). In Eq. (2), the updated bed elevations are used in TELEMAC-2D to estimate the hydrodynamic variables, which are sent back into SISYPHE to continue the simulation. Governing equations of TELEMAC-2D and erosion and deposition estimation in SISYPHE are described in the Supplementary material.

### 3.4. Model setup and boundary conditions

We simulated the flow and suspended sediment transport in the upper Tien and Hau Rivers (Figs. 1 and 3). The computational domain included a 200–300 m wide floodplain extending from both banks of the



**Table 1**  
Physical parameters of cohesive suspended sediment in previous publications that were used to tune our coupled model.

Parameters				References
$\omega_s$ (m/s)	$u_{cr}$ (m/s)	$M$ kg/(s·m <sup>2</sup> )	$\tau_{ce}$ (N/m <sup>2</sup> )	
$10^{-4}$ – $3 \times 10^{-4}$	$8.9 \times 10^{-3}$ – $1.1 \times 10^{-2}$	$5 \times 10^{-6}$ – $1 \times 10^{-4}$	0.15–1.5	Letrung et al., 2013
$2.16 \times 10^{-4}$ – $1.85 \times 10^{-3}$	$4.5 \times 10^{-3}$ – $5.3 \times 10^{-3}$	$5.13 \times 10^{-6}$ – $8 \times 10^{-6}$	0.028–0.044	Hung et al., 2014b
$10^{-4}$ – $1.3 \times 10^{-3}$	$4.4 \times 10^{-3}$ – $5 \times 10^{-3}$			Manh et al., 2014
$5 \times 10^{-5}$ – $3.3 \times 10^{-4}$	1.0	$2 \times 10^{-5}$	0.2	Thanh et al., 2017

ivers and all islands. The unstructured finite element triangle mesh was generated with a typical element size equal to 80 m in the main rivers, islands and floodplains and 30–40 m in the narrow channels. The domain consisted of 106,413 nodes and 206,455 elements. A time step of 10 s was selected to keep the Courant number <0.78 for model stability.

There were four boundaries: two upstream boundaries (i.e., Tan Chau and Chau Doc) used hourly flow discharges and daily SSCs, and two downstream boundaries (i.e., My Thuan and Can Tho) used hourly water levels (Fig. 3). The hourly discharge and water level were used because of the tidal effect. The initial riverbed material fractions were 95 % noncohesive sediment (fine sand) and 5 % cohesive sediment (Gugliotta et al., 2017). Uniform diameters of  $d_{50} = 12.6 \mu\text{m}$  (from our first field survey in 2017) and  $d_{50} = 214 \mu\text{m}$  (Gugliotta et al., 2017) were used for the cohesive and noncohesive sediments, respectively. The initial geometry was the 2014 river bathymetric data (we also used the 2010 and 2012 bathymetric data in the Hau River because of data availability) collected from the Southern Institute of Water Resources Research, Vietnam, and the 2013 SRTM floodplain topography. The model performance was evaluated using coefficient of determination ( $R^2$ ), Nash-Sutcliffe efficiency (NSE), and root mean square error (RMSE) (see Supplementary material).

### 3.5. Model calibration and validation

The VMD model was calibrated and validated using the data from 2014 to 2015 and 2016–2017, respectively. For each year, the model simulated seven months in the flood season from June to December to reduce the simulation time because >90 % of the suspended sediment was conveyed during the flood season (Binh et al., 2020b). In fact, June and December have relatively low discharges that are compatible with the dry season discharges, indicating that our model partially covered the dry season flow. Manning coefficients ranging from 0.016 to 0.034 were used initially, as recommended by Manh et al. (2014). Initial selections of other parameters were based on various publications, as shown in Table 1. We used water levels at Vam Nao, Cao Lanh, and Long Xuyen (as the discharges were not available), SSCs at Vam Nao, and riverbed elevations at six cross-sections (i.e., CS-1–CS-6) (Fig. 3a) to calibrate and validate the model.

We first calibrated the single hydrodynamic module TELEMAC-2D by adjusting the Manning coefficients and velocity diffusivity. We then recalibrated the coupled TELEMAC-2D/SISYPHE model by further tuning the reference near-bed concentration ( $z_{ref}$ ), the critical bed shear stress for erosion ( $\tau_{ce}$ ), the critical shear velocity for mud deposition ( $u_{cr}$ ), the settling velocity of the cohesive material ( $\omega_s$ ), and the Krone-Partheniades erosion constant ( $M$ ), together with a slight modification of the hydrodynamic tuning parameters. Manning coefficients were set by zones, namely,  $0.15 \text{ m}^{1/3}/\text{s}$  in the floodplains and islands based on the suggestion of Mtamba et al. (2015) and  $0.015$ – $0.04 \text{ m}^{1/3}/\text{s}$  in the river channels. In the sediment transport module,  $\tau_{ce} = 0.15 \text{ N/m}^2$ ,  $u_{cr} = 0.03 \text{ m/s}$ ,  $\omega_s = 6.6 \times 10^{-5} \text{ m/s}$ , and  $M = 10^{-6} \text{ kg/(s·m}^2)$ . The selected  $\omega_s$  was slightly larger than the value we measured at My Thuan because the sediment grain sizes were coarser in the upstream areas of this site (Hung et al., 2014b). The reference elevation  $z_{ref}$  was 2.5 times the median diameter of the noncohesive sediment. Values of RMSE, NSE,

**Table 2**  
Evaluation of the model performance.

Stations	Water levels			SSCs		
	RMSE (m)	NSE	$R^2$	RMSE (g/L)	NSE	$R^2$
Model calibration						
Vam Nao	0.10	0.83	0.90	0.02	0.72	0.87
Cao Lanh	0.09	0.94	0.94			
Long Xuyen	0.07	0.95	0.97			
Model validation						
Vam Nao	0.12	0.80	0.88	0.05	0.68	0.78
Cao Lanh	0.08	0.93	0.93			
Long Xuyen	0.06	0.97	0.98			

and  $R^2$  (Table 2) indicate that the coupled model was reliably calibrated and validated. Moreover, the simulated water levels, SSCs and riverbed elevations were in good agreement with the corresponding measured data (Fig. 4).

### 3.6. Simulated scenarios

Hydropower dams are the dominant driver of suspended sediment reduction and riverbed incision along the Mekong River (e.g., Lu and Siew, 2006; Kummur and Varis, 2007; Kummur et al., 2010; Kondolf et al., 2014b; Manh et al., 2015; Jordan et al., 2020; Binh et al., 2020b, 2021; Schmitt et al., 2021), together with sand mining (Brunier et al., 2014; Park et al., 2020; Gruel et al., 2022) and shifting in tropical cyclones (Darby et al., 2016). In this study, we did not focus on the drivers of morphological changes (see the work by Jordan et al. (2020)). Instead, we focused more on the morphodynamic processes and the quantification of the effects of the suspended sediment supply reductions by dams under three likely scenarios (Table 3). We simulated morphological changes for a ten-year period from 2017 to 2026 by considering the tradeoff between the model simulation time and morphological responses after upstream dam construction (15 years after Nuozhadu—the last largest mega dam in the Mekong basin). Scenario 1 (S1) used the flow and suspended sediment data of 2017, which were assumed to be unchanged until 2026. S1 was used as a baseline scenario. Scenarios 2 (S2) and 3 (S3) used the same flow conditions of 2017 until 2026, while the imposed inflow SSCs were reduced. Based on the long-term monthly suspended sediment reduction at Tan Chau plus Chau Doc analysed by Binh et al. (2020b), daily SSCs from 2017 to 2026 at the upstream boundaries at these two stations in S2 were estimated. Kondolf et al. (2014b) estimated that the SSL of the Mekong Delta would be only 4 % of that in the predam period (pre-1992) if all 133 planned dams in the Mekong Basin were built. This means that the post-133-dam SSL will be 6.7 Mt/yr (Binh et al., 2021). Compared to the 2017 SSL of 43.9 Mt, the 2026 SSL in S2 and S3 is reduced by 17.5 % and 84.8 %, respectively.

## 4. Results and discussions

### 4.1. Observed and simulated river flow dynamics

The flow regimes of the Tien and Hau Rivers show strong seasonality: high flows during July–December and low flows during January–June

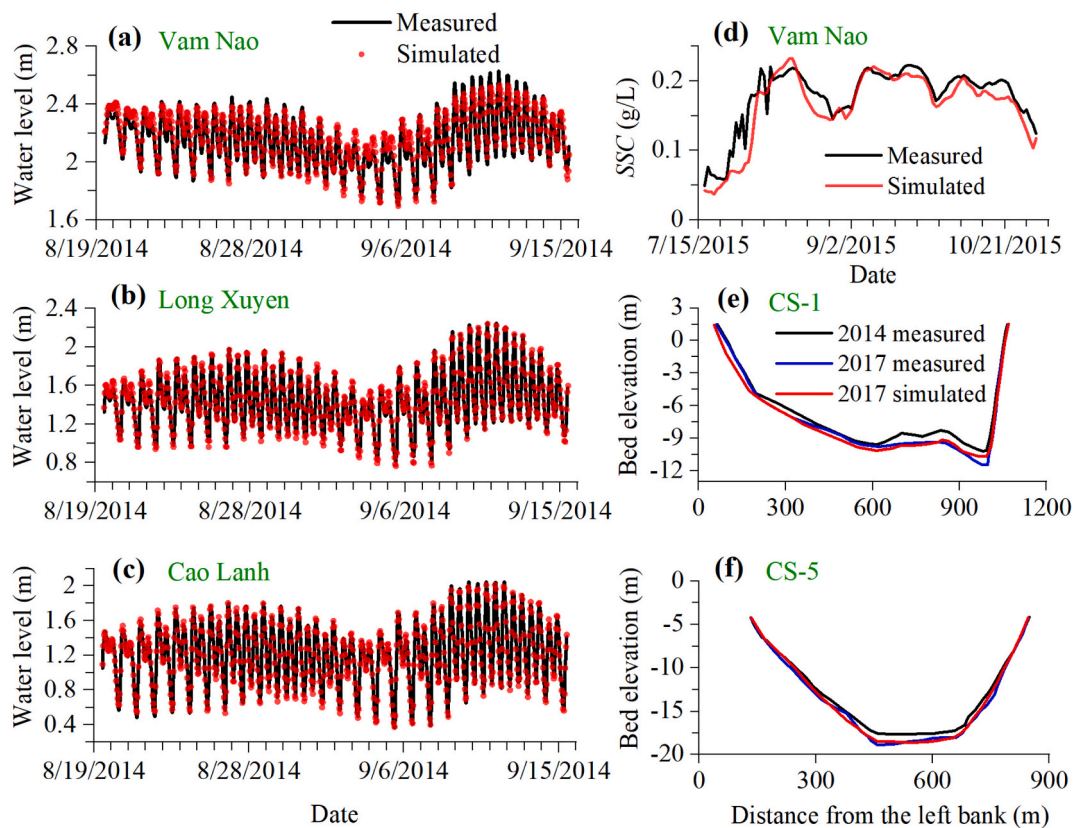


Fig. 4. Measured versus simulated water levels, SSCs, and riverbed elevations at various locations for (a–d) model calibration and (e–f) model validation. The locations indicated in the figure are shown in Fig. 3.

Table 3

Simulated scenarios in the coupled model to forecast morphological changes from 2017 to 2026 caused by suspended sediment reductions due to river damming.

Scenario	Discharge (m <sup>3</sup> /s)	Water level (m)	SSC (g/L)	SSL change (%) (2026 vs. 2017)
S1	Same as 2017	Same as 2017	Same as 2017	–
S2	Same as 2017	Same as 2017	Based on long-term monthly suspended sediment reduction in Binh et al. (2020b) 2017	–17.5 %
S3	Same as 2017	Same as 2017	Based on Kondolf et al. (2014b) 2017 → 2019 ↓ 2020 → 2026	–84.8 %

(Figs. 5a–b and 6). The observed daily flood peaks at Tan Chau and Chau Doc were large in 2014, corresponding to maximum daily discharges of 24,350 and 6620 m<sup>3</sup>/s (water levels of 3.71 m and 2.95 m), respectively. However, due to (mainly) the redistribution of flow by the Vam Nao diversion channel, the simulated daily flood peaks at Long Xuyen and Cao Lanh in 2014 were 18,930 and 16,230 m<sup>3</sup>/s, respectively. During the period from 2014 to 2017, the observed data show that the mean annual flow ratio between the Tien and Hau Rivers upstream of the Vam Nao channel (i.e., at Tan Chau and Chau Doc) was 83:17, while that downstream of the Vam Nao channel (from simulated results at Cao Lanh and Long Xuyen) was 52:48. This analysis indicates that the Vam Nao diversion channel may have a significant impact on the flow dynamics of the Tien and Hau Rivers.

The observed and simulated discharges from 2014 to 2017 during the dry season (March–April) show that the flow direction was reversed (Figs. 5a and 7), with maximum hourly rates of –4780 m<sup>3</sup>/s and –1850 m<sup>3</sup>/s (in 2016) at Tan Chau and Chau Doc, respectively (Fig. 5a). This is because of the tidal effect, which causes the tidal discharge to exceed the

low riverine flow. In the dry year (i.e., 2016), the observed mean annual discharge at My Thuan was lower than that at Can Tho, with a ratio of 48:52. This indicates that the tidal effect may be stronger in the Hau River than in the Tien River (Fig. 5b). Both observed and simulated data show that the tidal regime may have had a clear effect on the water levels of the two rivers (Figs. 4a–c and 5b). This is illustrated by a sinusoidal oscillation of the water levels in these rivers, which mimics changes in the tidal regime.

The observed data show that the vertical distribution of the flow velocity largely depended on the shape of the cross-section (Fig. 5c–d). In asymmetric cross-sections (Fig. 5c), the flow was faster on the steeper bank, whereas in symmetric cross-sections (Fig. 5d), the velocity was symmetric. The velocity was generally larger in the upper zone than in the lower zone in a cross-section. During the flood peak, the simulated maximum flow velocity exceeded 2 m/s in some areas, especially in narrow and meandering sections (Fig. 6c), resulting from high unit discharges (Fig. 6a). On the other hand, the simulated dry season flow velocities were mostly smaller than 1.5 m/s (Fig. 6f). However, the

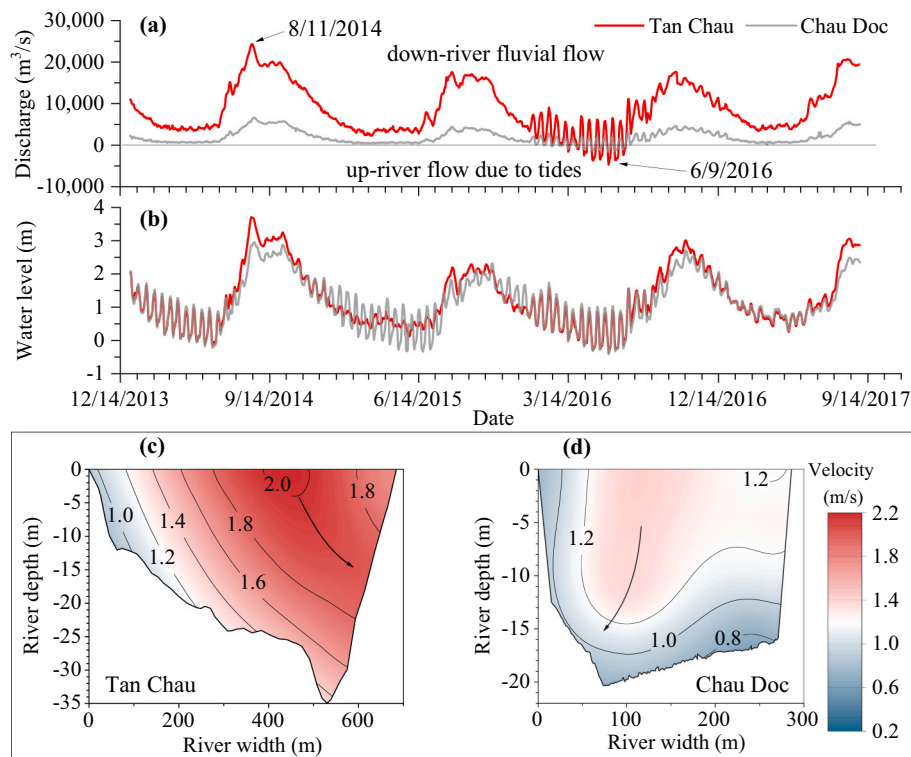


Fig. 5. Observed hydraulic conditions at Tan Chau and Chau Doc: a) daily discharge and b) water level from 2014 to 2017. Vertical velocity distribution at c) Tan Chau and d) Chau Doc measured in August 2017 (flood season) during the first field survey.

pattern of the simulated water depth in the dry season was similar to that in the flood season (Fig. 6b, e).

#### 4.2. Suspended sediment dynamics and distribution

Suspended sediment in the VMD varies inter- and intra-annually (Figs. 8–9). The observed and simulated maximum daily SSC (from the gauging stations at Tan Chau to Vam Nao) during the flood season (i.e., August–September) reached 0.47 g/L (equivalent to almost 1 Mt), while the minimum value during the dry season (i.e., March–April) was negligible. Most of the suspended sediment was transported during the flood season: 90–98 % at Tan Chau, 91–96 % at Chau Doc, 89–93 % at My Thuan, and 86–94 % at Can Tho during 2014–2017 (Fig. 8b–e). Although the maximum SSL of the VMD during 2014–2017 was 66 Mt/yr (in 2014), this value was lower than the predam SSL (pre-1992) of 166.7 Mt/yr (Binh et al., 2020b). On average, the mean annual SSL of the VMD in 2014–2017 (42 Mt/yr) decreased by approximately 75 % compared to the predam amount. Because hydropower dams are likely to contribute to a significant reduction in the SSL in the VMD (Binh et al., 2020b), a sustainable reservoir sediment management plan should be implemented for current and planned dams in the Mekong basin. For existing dams, prompt measures (i.e., excavation) can be considered to urgently dredge the accumulated sediment in reservoirs for delivery downstream. For planned dams, alternative locations and designed configurations of dams should be revised to minimize reservoir sedimentation. Then, conventional sediment management measures (e.g., drawdown flushing, bypassing, and sluicing) to route sediment through or bypass reservoirs should be considered at the design stage. Furthermore, advanced sediment management techniques, such as hydro-suction, dam asset management, and dam rehabilitation and retrofitting, can be employed. Schmitt et al. (2021) found that it is very important to consider strategic placement of hydropower dams to maintain sediment supply from the Mekong basin rather than trying to increase sediment yields or improve sediment management for individual dams.

There are substantial differences in the spatial variations in the suspended sediment between the flood and dry seasons (Figs. 8–9). In dry seasons, the simulated SSLs along the rivers were relatively similar because of the low supply of suspended sediment from the Mekong River (Fig. 9a) and the high SSC induced by tides and wind (Thanh et al., 2017; Xing et al., 2017; Eslami et al., 2019). However, during flood seasons, the simulated results show that the SSC decreased in the downstream direction because of the high suspended sediment supplied from the Mekong River (Fig. 9b). In the Hau River, the observed mean suspended sediment ratios between Can Tho and Chau Doc from 2014 to 2017 were 3.2–5.6 and 1.6–3.1 during the dry and flood seasons, respectively. The mean ratio in 2009 estimated by Manh et al. (2014) was 2.8. These results imply that the sediment flux of the Mekong River in the flood season may play a key role in stabilizing landforms in the VMD estuaries, especially in compacting with the shrinkage of the delta due to rapid coastal and riverbank erosion (Li et al., 2017; Khoi et al., 2020). The newly deposited suspended sediment in the floodplains carried by the Mekong's flood flows may also help counteract the delta's sinking resulting from relative land subsidence (i.e., absolute land subsidence plus rising sea level) due to groundwater overexploitation (Minderhoud et al., 2020; Tran et al., 2021). However, the sediment load of the Mekong River has been reducing due to human activities (Kondolf et al., 2014b) and tropical cyclone shifts (Darby et al., 2016). To address this issue, Schmitt et al. (2021) suggested maintaining the sediment supply from the Mekong basin in enhancing climate resilience and maintaining lands in the delta.

Both the observed and simulated SSC and SSL in the Tien River were significantly greater than those in the Hau River (Figs. 8–9). The observed mean annual suspended sediment ratios between the Tien and Hau Rivers during 2014–2017 were 84:16 and 61:39 upstream (i.e., Tan Chau and Chau Doc) and downstream (i.e., My Thuan and Can Tho) of the Vam Nao diversion channel, respectively. This difference between the upstream and the downstream is likely because of the Vam Nao channel, which diverts large amounts of water and suspended sediment



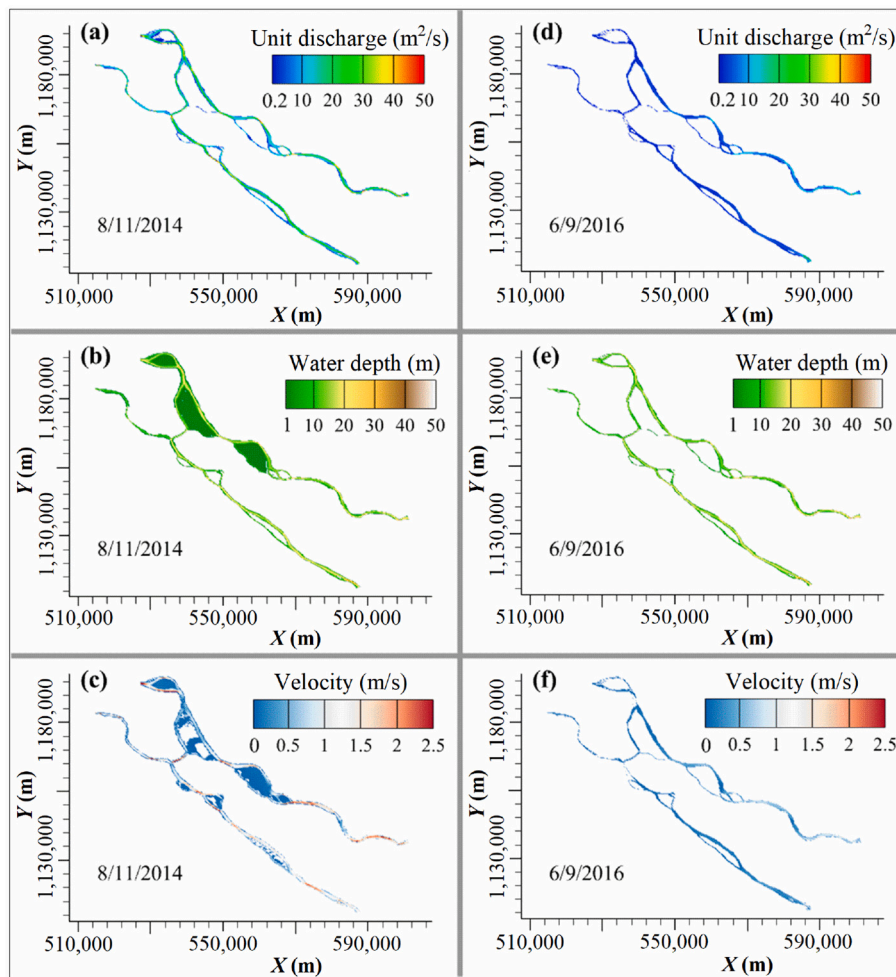


**Fig. 6.** Simulated unit discharge, water depth, and velocity magnitude (a–c) during the annual flood peak on 8/11/2014 and (d–f) during the nonflood period on 6/9/2016. For clarity, we applied cut-offs of 0.2 m<sup>2</sup>/s, 1 m, and 0.02 m/s to the maps showing the unit discharge, water depth, and flow velocity, respectively.

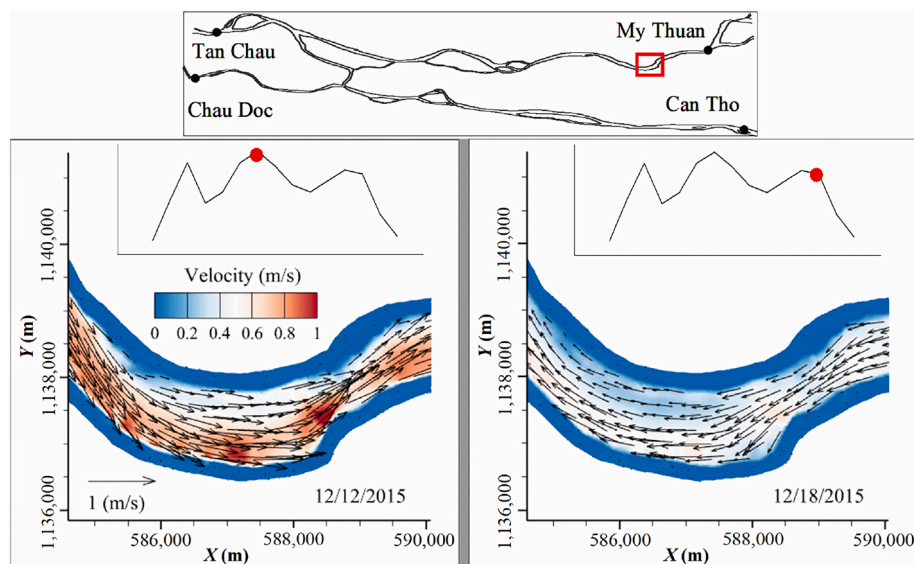


**Fig. 7.** Simulated magnitude and direction of flow velocity, showing reversed flow caused by tidal effects under low riverine fluvial discharge. The sketch on the top indicates the study area.

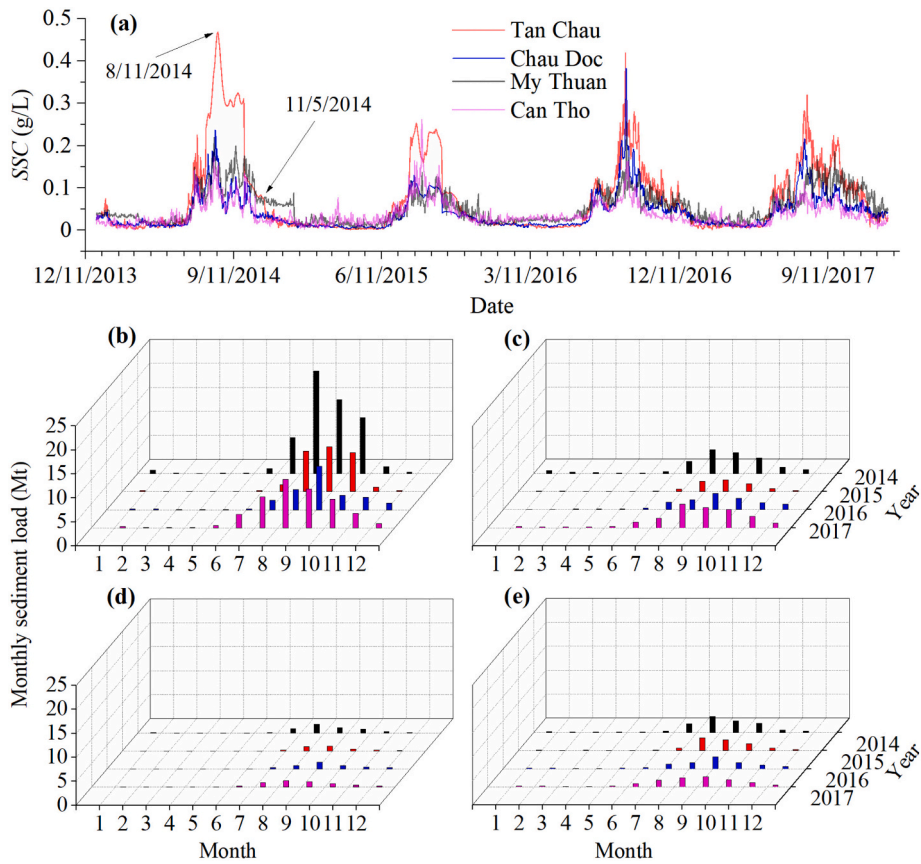


Fig. 8. Observed (a) daily SSC in the VMD and monthly SSL at (b) Tan Chau, (c) Chau Doc, (d) My Thuan, and (e) Can Tho.

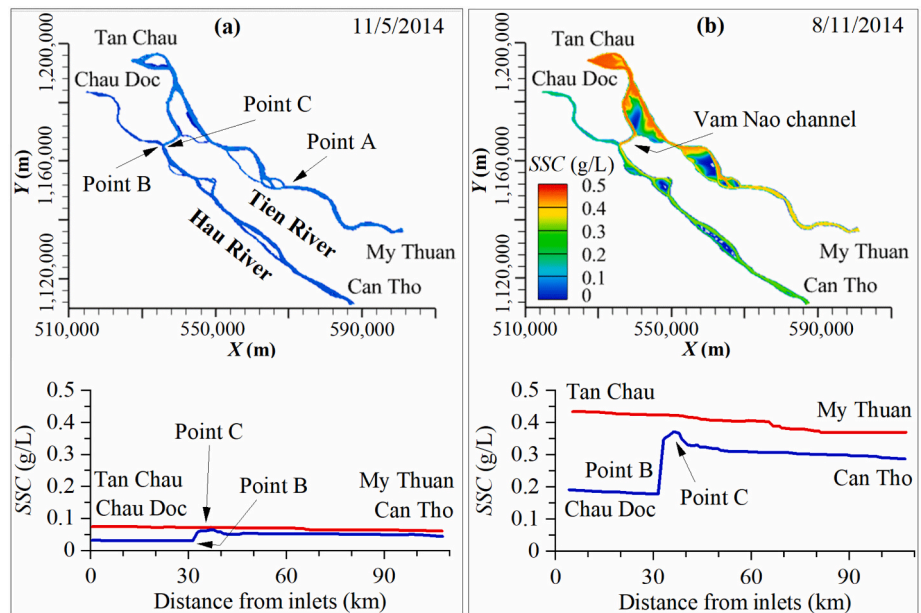
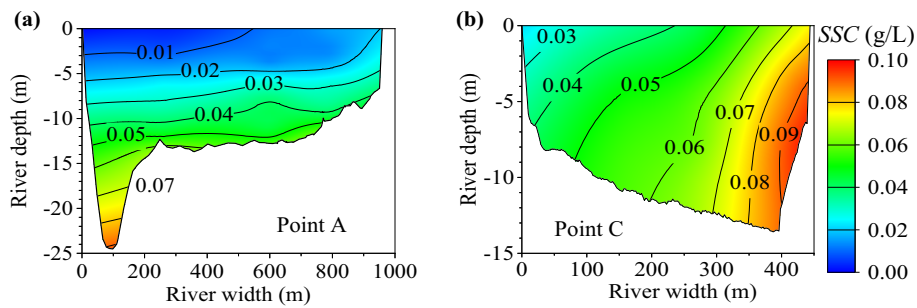


Fig. 9. Spatial and longitudinal distribution of the simulated SSC in (a) nonflood conditions on 11/5/2014 and (b) flood conditions on 8/11/2014. Longitudinal SSCs are extracted along the main branches of the Tien and Hau Rivers.

from the Tien River to the Hau River. Suspended sediment diverted from the Tien River to the Hau River via the Vam Nao channel (mainly in the flood season) can be attributed to a significant discharge difference between the two rivers upstream of this diversion channel (i.e., 83 % in the Tien River and 17 % in the Hau River, see Section 4.1). Such a large

discharge difference may create a hydraulic gradient from the Tien River towards the Hau River, leading to a sharing of suspended sediment from the former to the latter that balances the suspended sediment budget and geomorphological conditions in the VMD's river network. Fig. 9 clearly shows that the simulated SSC in the Hau River above Point B was very



**Fig. 10.** Observed vertical distribution of SSC at (a) the cross-section at Point A (35 km from My Thuan) in which a scour hole appeared on the left bank and (b) the cross-section at Point C (located at the Vam Nao channel-Hau River confluence, 1 km downstream from Point B) in April 2018 (dry season) during our field survey. The locations of Points A and C are shown in Fig. 9.

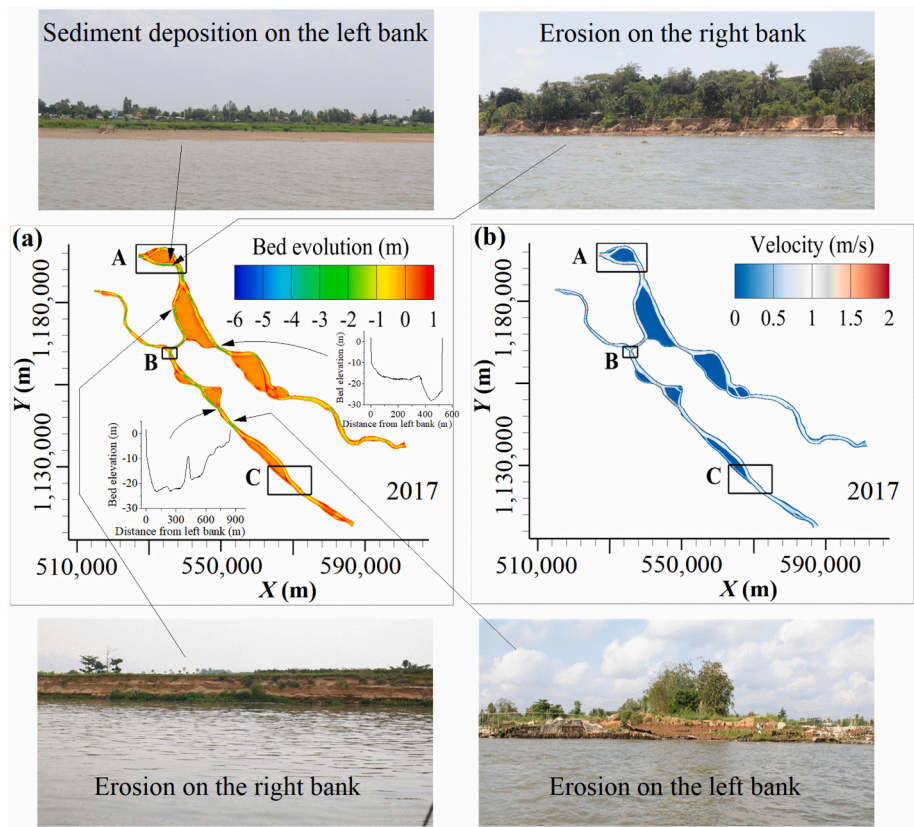


**Fig. 11.** Simulated riverbed evolution in 2017 compared to the 2014 riverbed level: (a) spatial evolution depth and (b) velocity magnitude. The modelled scour holes are typically compared with the scour holes in cross-sections measured in September 2017 during the first field survey (Fig. a) to illustrate the prediction reliability. Some typical locations of riverbank erosion and deposition are shown by photos taken during the second field trip in April 2018. Details of Zones A–C are shown in Fig. 12.

low and suddenly increased from Point B to Point C. In particular, approximately 61–81 % of the monthly SSL during flood seasons from 2014 to 2017 at Point C was from the Vam Nao channel. These percentages are in line with the estimate of 76 % in 2009 by Manh et al. (2014). This indicates that the Vam Nao channel is very important in balancing water and suspended sediment in the VMD river system. Any changes in the morphology of the Vam Nao channel (discussed in Section 4.3) may cause changes in the total water and suspended sediment budgets in the delta. Therefore, maintaining the geomorphological stability of the Vam Nao channel may favour the sustainable development of the VMD.

Fig. 10 shows the vertical distribution of the observed SSC, which depended on the shape of the cross-section and flow pattern. The SSC was always higher in the lower layer than in the upper layer, on the order of 2 or 3 times. The sediment tends to be trapped in the scour holes, resulting in higher SSCs in cross-sections at such locations (Fig. 10a). The SSC in the scour hole was approximately 8 times greater

than that at the surface. In an asymmetric cross-section, the SSC was higher on the steeper-slope bank than on the opposite bank. For instance, the SSC on the right bank in Fig. 10b was more than double that on the left bank. This is likely because of the higher flow velocity, which has a larger capacity to transport and erode sediment from the bank.

#### 4.3. Riverbed evolution and scour hole formation

Fig. 11 shows the simulated riverbed changes from 2014 to 2017. Generally, the riverbed of the Vam Nao channel was highly incised compared to those of the Tien and Hau Rivers. Riverbed incision mainly occurred on the outer banks of meanders, at confluences, and in the middle of the narrowing (contracted) channels (Figs. 11a and 12a–b), where the flow velocity was high (Fig. 11b). On the other hand, deposition mostly appeared on the inner banks of meanders, on the tail of islands, and in secondary channels (Figs. 11a and 12c), where the



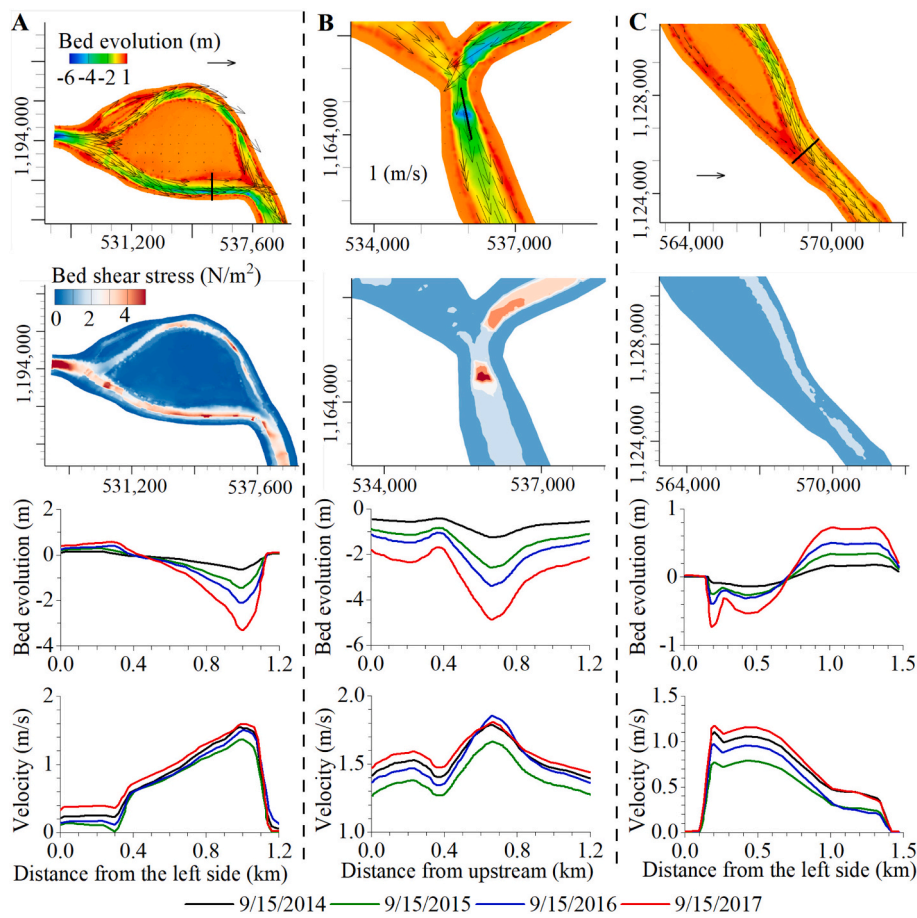


Fig. 12. Typical locations of riverbed evolution (e.g., at scour holes) during the simulated 2014–2017 period and associated bed shear stress (average over 2014–2017 period) and flow velocity distributions. The locations of Zones A–D are shown in Fig. 11.

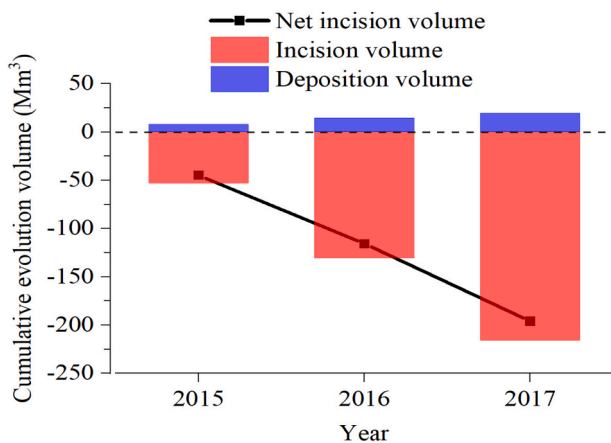


Fig. 13. Simulated cumulative riverbed erosion and deposition volume of the entire study area. The riverbed experiences annual net erosion.

velocity was low. In the Tien River, most of the riverbed incision sections were from Tan Chau to Vam Nao and from Cao Lanh to My Thuan. These most significant incision sections were also reported by Binh et al. (2020b) and Jordan et al. (2019) based on measured bathymetric data. In the Hau River, the riverbed was more incised from Chau Doc to Long Xuyen.

The simulated mean net riverbed incision depths of the Vam Nao, Tien, and Hau Rivers were  $-2.38$ ,  $-1.12$ , and  $-0.68$  m, respectively, from 2014 to 2017. These values corresponded to incision rates of 0.79,

0.37, and 0.23 m/yr, respectively. The simulated results show that the mean cumulative incision volume of the entire study area from 2014 to 2017 was  $-65.3 \text{ Mm}^3/\text{yr}$  (Fig. 13), which was underestimated by 22.4 % compared to the measured volume of  $-84.1 \text{ Mm}^3/\text{yr}$  in the same period. The model underestimates the incision volume and depth because the sand mining effect was not accounted for in our model. Sand mining accounted for 25.6 % of the total incision volume (Binh et al., 2021). Moreover, model uncertainty may partially contribute to such an underestimation. Conversely, riverbed incision in 2017 was the most significant ( $85.2 \text{ Mm}^3$  incision compared to only  $5.1 \text{ Mm}^3$  deposition) (Fig. 13) because of its high flood flow (Fig. 5a) and relatively low SSC (Fig. 8a). Additionally, the total net simulated incision volume of the entire study area was  $-196 \text{ Mm}^3$  from 2014 to 2017, which was on the same order as  $-200 \text{ Mm}^3$  over the ten-year period of 1998–2008 in the entire VMD estimated by Brunier et al. (2014).

According to Fig. 14a–b, the model predicted the formation of nine scour holes in the Tien River and seven scour holes in the Hau River. The riverbed will be identified as a scour hole if the slope of the riverbed at the scour zone is suddenly steeper than the slope of the surrounding areas; the mean ratio of the slopes between the scour holes and the surrounding areas was, on average, approximately 15 times. The modelled scour hole locations were verified by comparing them with those measured during the first field survey in September 2017 (Fig. 11a). We classified scour holes into three categories according to the scour depths (i.e., at the deepest point), namely, shallow (scour depths  $<5$  m), medium (scour depths from 5 m to 10 m), and deep (scour depths  $>10$  m), based on percentiles of approximately 33 %. Under this consideration, two scour holes in the Tien River and one scour hole in the Hau River were classified as medium, whereas the remaining scours

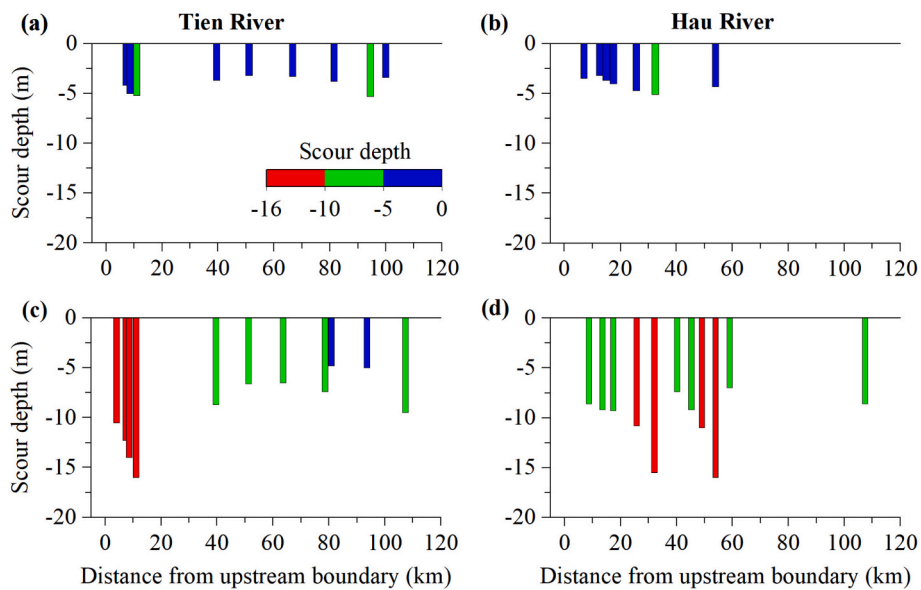


Fig. 14. Classifications of scour holes based on the scour depth (the bar charts) and geomorphological settings (pie charts) during 2014–2017 (a–b) and in scenario 3 during 2017–2026 (c–d).

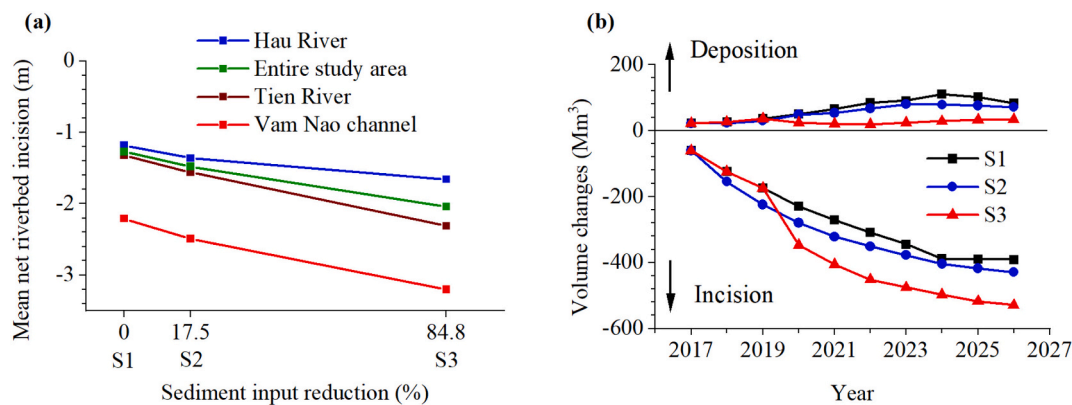


Fig. 15. Predicted morphological changes in the three scenarios: (a) mean net riverbed incision depth and (b) annual total volume changes in the entire study area.

were shallow.

We found that most of the scour holes were formed at river confluences and meandering segments. Although the processes of scour hole formation were different in these geomorphological settings (Rice et al., 2008; Ferrarin et al., 2018), the common mechanism was that the erosive capacity of the flow was very high in the scour holes because of the high flow velocity, which induced high bed shear stresses. In this study, we neglected the small-scale processes in scour holes. Representative simulated scour holes at Zones A and B are illustrated in Fig. 12a–b. In these scour holes, the incision rate was largest in 2017 when high flood flow was combined with low SSC (Figs. 5a and 8a). Notably, the scour hole at Zone B was at the location of a severe riverbank collapse that occurred on 22 April 2017 (Binh et al., 2020b). Therefore, we speculate that scour holes are likely one of the main causes of riverbank erosion in the VMD that local authorities should consider in their protective actions against riverbank collapse.

#### 4.4. Forecasted morphological changes between 2017 and 2026 due to sediment reductions

Riverbeds in the VMD were forecasted to be significantly incised by 2026 (Fig. 15). The mean net riverbed incision depths of the Tien, Hau, and Vam Nao Rivers in S1 were  $-1.32$ ,  $-1.18$ , and  $-2.21$  m,

respectively. The respective values were  $-1.56$ ,  $-1.36$ , and  $-2.49$  m in S2 and  $-2.31$ ,  $-1.66$ , and  $-3.2$  m in S3. We found that the forecasted riverbed incision in the Vam Nao channel was higher than that in the Tien and Hau Rivers (Fig. 15a). Upstream of the Vam Nao channel, the riverbed of the Tien River was more incised than that of the Hau River, but the opposite was true downstream of the Vam Nao channel. The forecasted riverbed incision of both the Tien and Hau Rivers was more severe upstream than downstream of the Vam Nao channel. We estimated that the total net bed sediment losses from 2017 to 2026 in the entire study area were  $-2472$  and  $-3316$  Mm<sup>3</sup> in scenarios S2 and S3, respectively, which were increased by 23 % and 65 % compared to S1 ( $-2011$  Mm<sup>3</sup>) (Fig. 15b). On average, the forecasted mean net riverbed incision by 2026 of the entire study area was increased by 17 % and 61 % in S2 ( $-1.48$  m) and S3 ( $-2.04$  m), respectively, compared to S1 ( $-1.27$  m) (Fig. 15a). The projected increasing riverbed incision may in turn cause some resulting environmental changes in the VMD. First, it may intensify salinity intrusion, causing difficulties in people's livelihoods (Loc et al., 2021). This may require a large-scale economic transformation (i.e., plants and animals that can survive under high salinity concentrations) for the system to adapt to changing conditions. Second, the incised riverbed may also reduce water levels during dry seasons, causing difficulty for irrigation because of river–floodplain disconnection (Park et al., 2020; Binh et al., 2021).

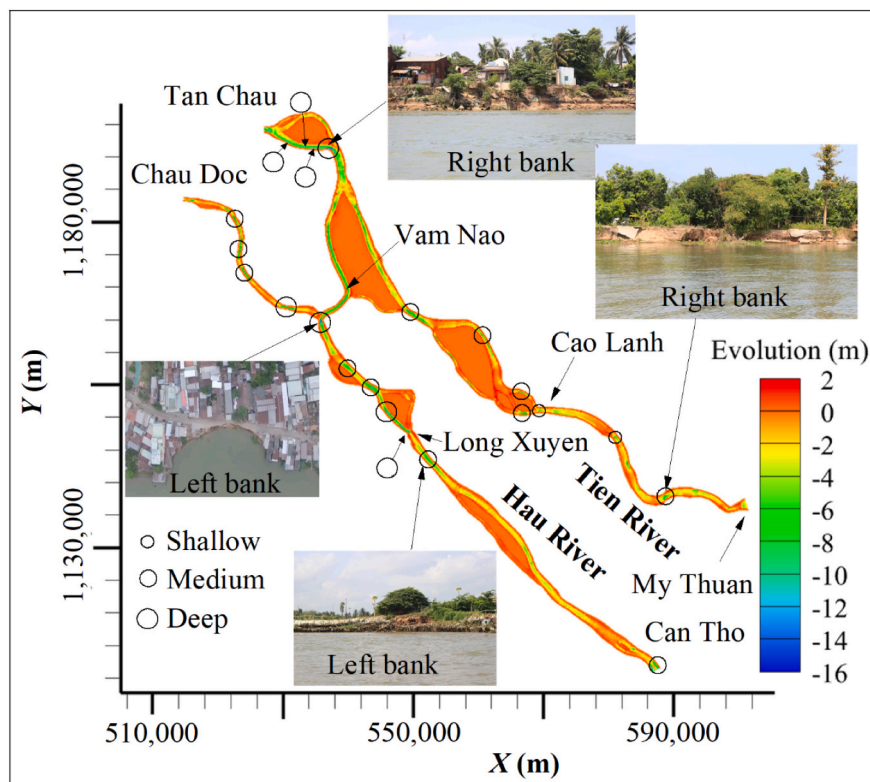


**Fig. 16.** Forecasted riverbed evolution in 2026 relative to 2017 in S3 under an 84.8 % suspended sediment reduction. Twenty-two scour holes (indicated by black circles) are formed. Some of the scour holes are at the locations of riverbank erosion observed during the 2018 field survey. A drone photo of a severe bank collapse at the Hau River-Vam Nao channel confluence was retrieved from [Vnexpress.net](https://vnxpress.net) accessed on 1/18/2021.

During 2017–2026, twenty-two large-scale scour holes were forecasted to form in the Tien and Hau Rivers in S3, 11 in each (Fig. 16). The scour depths in S3 became deeper than those in 2014–2017. In the Tien River, four scour holes were classified as deep and five as medium (Fig. 14c). In the Hau River, four scour holes were classified as deep and seven as medium (Fig. 14d). The most severe scour hole was likely at the Hau River-Vam Nao channel confluence (Figs. 14d and 16). The maximum scour depth at this location in S3 was forecasted to be up to  $-16$  m by 2026. In the Tien River, the most severe scour hole was likely at a location 11 km downstream from Tan Chau, at which the riverbank was eroded (Figs. 14c and 16). Notably, our forecasted riverbed incision at this location was likely underestimated because we did not account for the sand mining effect in our model, while sand mining was very active there (Fig. 1b). Generally, the forecasted severe scour holes were around the locations of severe riverbank erosion observed during our field surveys in 2018 (Fig. 16). Therefore, it is likely that scour holes will continue to cause the increasing collapse of the riverbank in the near future.

Although not included in the model, sand mining remains one of the key causes of riverbed incision in the VMD (Brunier et al., 2014; Gruel et al., 2022). Scour holes formed by sand mining are likely to trap the bedload, which may result in a deficit in the bedload supply to the downstream reaches, likely causing migration/expansion of riverbed incision in both upstream and downstream directions (Anh et al., 2022). Moreover, scour holes created by sand mining can be a root cause of riverbank instability (Hackney et al., 2020). This can explain why the scour holes predicted by our model were near the locations of severe riverbank erosion (Figs. 11 and 16). To alleviate/decelerate the likely consequences of riverbed incision and scour holes on river system stability, in addition to considering integrated sediment management at the basin scale, including sustainable reservoir sedimentation management, sand mining should be strictly prohibited in the VMD with stronger regulations to prevent illegal mining activities, both from licensed

operators and from local citizens. Decision makers are recommended to take actions to limit sand mining activities (i.e., considering not relicensing the expired mining sites while not approving new licenses) to save our delta in the long run.

#### 4.5. Model uncertainties and outlook

The developed model may encounter some uncertainties. First, the 2014 bathymetric data are not fully available for the entire Hau River. Therefore, the bathymetric data measured in 2010 and 2012 were also used to create the input geometry. However, these data are up-to-date. Second, the model did not include sand mining effects on morphological changes. Thus, the simulated mean net riverbed incision volume in the entire study area from 2014 to 2017 ( $-65.3 \text{ Mm}^3/\text{yr}$ ) was underestimated by 22.4 % compared to the measured data ( $-84.1 \text{ Mm}^3/\text{yr}$ ). This value is within the range of 14.8–25.6 % under sand mining effects on riverbed incision (Binh et al., 2020b, 2021). The underestimation can be attributed partially to sand mining (i.e., it is present in reality but was not considered by the model) and partially to model uncertainty. Third, bedload transport was not considered, which may lead to unavoidable uncertainty in bed evolution. However, this is acceptable because the bedload contributes a negligible amount (1–3 %) to the total load (Jordan et al., 2019; Hackney et al., 2020). Fourth, to reduce the simulation time, we simulated only seven months during the flood season in each simulated year. This may have uncertainties in the erosion and deposition processes. However, this consideration is appropriate because up to 98 % of the suspended sediment in the VMD is transported within the flood season (Fig. 8b–e). Fifth, the model used a sediment mixture of only two sediment classes (cohesive and non-cohesive), while the natural sediment is usually composed of different grain sizes (Lepesqueur et al., 2019). This simplification may result in under- or overestimation of bed evolution because the model neglects the effects of sediment densities and grain size distributions, which have



been proven to substantially enhance the performance of the model (Lepesqueur et al., 2019). Sixth, longer projected time scales (e.g., spanning several decades) should be forecasted to provide better information for holistic river management. Finally, drivers of riverbed incision are not only dams but also sand mining/dredging (Anh et al., 2022; Gruel et al., 2022) and climate variability/change (Darby et al., 2016). Therefore, future studies are expected to quantify the role of each driver on riverbed incision in the large-scale VMD, which can provide important indications for the government to sustainably develop the delta while effectively minimizing the negative impacts.

## 5. Conclusions

Hydrodynamics, suspended sediment transport, and morphodynamics in fluvial-dominated, tide-affected rivers in the VMD from 2014 to 2017 were investigated using field survey data and a coupled hydrodynamic and sediment transport model. The morphological evolution under three scenarios of suspended sediment supply reductions was forecasted for the decade ending in 2026. The main findings of this study are as follows:

- The Vam Nao channel has a significant impact on the flow and suspended sediment dynamics of the Tien and Hau Rivers. We estimated that approximately 61–81 % of the mean SSL of the Hau River was diverted from the Tien River via the Vam Nao channel in the flood season from 2014 to 2017.
- We found that the tidal effect was stronger in the Hau River than in the Tien River. Both observed and simulated data from 2014 to 2017 show that the tidal regime has a clear effect on the water level.
- In the Tien River during the dry season from 2014 to 2017, the SSL was longitudinally higher upstream than downstream of the Vam Nao channel due to tidal effects. However, the opposite relationship was observed during the flood season because of the dominance of the riverine fluvial flow from the Mekong River. In the Hau River, the SSL was always higher downstream than upstream of the Vam Nao channel because of suspended sediment diverted from the Tien River.
- The simulated results from 2014 to 2026 show that riverbed incision is higher in the Vam Nao channel than in the Tien and Hau Rivers. In the Tien River, the sections with the most riverbed incision are from Tan Chau to Vam Nao and from Cao Lanh to My Thuan. In the Hau River, the riverbed is more incised from Chau Doc to Long Xuyen.
- Simulated results show that 16 scour holes were formed in the Tien and Hau Rivers during 2014–2017. We forecasted that 22 scour holes are likely to appear in these rivers by 2026 if the suspended sediment supply from the Mekong River is reduced by 84.8 % due to river damming. Scour holes are predicted to be formed at locations of severe riverbank erosion observed during our field surveys in 2018. We anticipate that scour holes are likely to continue to cause increasing collapse of the riverbank in the near future. Therefore, the predicted results can provide useful information for local authorities to actively propose appropriate countermeasures against riverbank erosion.

## Declaration of competing interest

None.

## Acknowledgements

The authors would like to acknowledge the Mekong River Commission and the Vietnam National Center for Hydrometeorological Forecasting for providing the data. The data from the Mekong River Commission can be obtained from <https://www.mrcmekong.org/>. The Telemac-Mascaret modelling system can be freely downloaded at <http://www.opentelmac.org/>. The authors would like to acknowledge

Dr. Nguyen Thi Phuong Mai from Thuyloi University, Vietnam, for supporting us in conducting the field surveys and in collecting the flow data in the Vietnamese Mekong Delta. We are thankful to Mr. Nguyen Hoang Long, director of Hai Au Technology Joint Stock Company, and Mr. Take Toshiaki, adviser of JFE Advantech Co., Ltd., for supporting us with the Infinity turbidity and velocity meters and accompanying us in the 2018 field survey. This work was funded by the Japan-ASEAN Science, Technology and Innovation Platform (JASTIP), the Supporting Program for Interaction-Based Initiative Team Studies (SPIRITS) 2016 of Kyoto University, and the Asia-Pacific Network for Global Change Research under project reference number CRRP2020-09MY-Kantoush. This paper is based on a part of Doan Van Binh's doctoral thesis.

## Appendix A. Supplementary data

Supplementary data to this article can be found online at <https://doi.org/10.1016/j.geomorph.2022.108368>.

## References

- Anh, L.N., Tran, D.D., Thong, N., Van, C.T., Vinh, D.H., Au, N.H., Park, E., 2022. Drastic variations in estuarine morphodynamics in Southern Vietnam: investigating riverbed sand mining impact through hydrodynamic modelling and field controls. *J. Hydrol.* 608, 127572.
- Anthony, E.J., Brunier, G., Besset, M., Goichot, M., Dussouillez, P., Nguyen, V.L., 2015. Linking rapid erosion of the Mekong River Delta to human activities. *Sci. Rep.* 5, 14745.
- Best, J., 2019. Anthropogenic stresses on the world's big rivers. *Nat. Geosci.* 12, 7–21.
- Binh, D.V., Kantoush, S., Sumi, T., Mai, N.P., 2018. Impact of Lancang cascade dams on flow regimes of Vietnamese Mekong Delta. *Annu. J. Hydraul. Eng.* 74, 487–492.
- Binh, D.V., Kantoush, S.A., Saber, M., Mai, N.P., Maskey, S., Phong, D.T., Sumi, T., 2020a. Long-term alterations of flow regimes of the Mekong River and adaptation strategies for the Vietnamese Mekong Delta. *J. Hydrol. Reg. Stud.* 32, 100742.
- Binh, D.V., Kantoush, S., Sumi, T., 2020b. Changes to long-term discharge and sediment loads in the Vietnamese Mekong Delta caused by upstream dams. *Geomorphology* 353, 107011.
- Binh, D.V., Kantoush, S., Sumi, T., Mai, N.P., Trung, L.V., 2020. Dam-induced riverbed incision and saltwater intrusion in the Mekong Delta. In: Uijtewaal, W.S.J., Crosato, A., Schielen, R. (Eds.), *River Flow*. Taylor & Francis Group, London, UK.
- Binh, D.V., Wietlisbac, B., Kantoush, S., Loc, H.H., Park, E., de Cesare, G., Cuong, D.H., Tung, N.X., Sumi, T., 2020d. A novel method for river bank detection from Landsat satellite data: a case study in the Vietnamese Mekong Delta. *Remote Sens.* 12, 3298.
- Binh, D.V., Kantoush, A.A., Sumi, T., Mai, N.P., Ngoc, T.A., Trung, L.V., An, T.D., 2021. Effects of riverbed incision on the hydrology of the Vietnamese Mekong Delta. *Hydrol. Process.* 35, e14030.
- Boretti, A., 2020. Implications on food production of the changing water cycle in the Vietnamese Mekong Delta. *Glob. Ecol. Conserv.* 22, e00989.
- Bravard, J.-P., Goichot, M., Gaillot, S., 2013. Geography of sand and gravel mining in the lower Mekong River: first survey and impact assessment. *EchoGéo* 26, 1–18.
- Brunier, G., Anthony, E.J., Goichot, M., Provansal, M., Dussouillez, P., 2014. Recent morphological changes in the Mekong and Bassac River channels, Mekong Delta: the marked impact of river-bed mining and implications for delta destabilisation. *Geomorphology* 224, 177–191.
- Dang, T.D., Cochrane, T.A., Arias, M.E., Van, P.D.T., Vries, T.T.D., 2016. Hydrological alterations from water infrastructure development in the Mekong floodplains. *Hydrol. Process.* 30, 3824–3838.
- Dang, T.D., Cochrane, T.A., Arias, M.E., 2018. Quantifying suspended sediment dynamics in mega deltas using remote sensing data: a case study of the Mekong floodplains. *Int. J. Appl. Earth Obs. Geoinf.* 68, 105–115.
- Darby, S.E., Hackney, C.R., Leyland, J., Kumm, M., Lauri, H., Parsons, D.R., Best, J.L., Nicholas, A.P., Aalto, R., 2016. Fluvial sediment supply to a mega-delta reduced by shifting tropical-cyclone activity. *Nature* 539, 276–279.
- El kadi Abderrezzak, K., Die Moran, A., Tassi, P., Ata, R., Herouvet, J.M., 2016. Modelling river bank erosion using a 2D depth-averaged numerical model of flow and non-cohesive, non-uniform sediment transport. *Adv. Water Res.* 93, 75–88.
- Eslami, S., Hoekstra, P., Trung, N.N., Kantoush, S.A., Binh, D.V., Dung, D.D., Quang, T.T., van der Vegt, M., 2019. Tidal amplification and salt intrusion in the Mekong delta driven by anthropogenic sediment starvation. *Sci. Rep.* 9, 18746.
- Exner, F.M., 1925. Über die Wechselwirkung zwischen Wasser und Geschiebe in Flüssen. *Akad. Wiss. Wien Math. Naturwiss. Klasse* 134, 165–204.
- Ferrarin, C., Madricardo, F., Rizzetto, F., Kiver, W.M., Dellafiore, D., Umgiesser, G., Kruss, A., Zaggia, L., Fogliani, F., Ceregato, A., Sarretta, A., Trincardi, F., 2018. Geomorphology of scour holes at tidal channel influences. *J. Geophys. Res. Earth Surf.* 123, 1386–1406.
- Gruel, C.R., Park, E., Switzer, A.D., Kumar, S., Ho, H.L., Kantoush, S., Binh, D.V., Feng, L., 2022. New systematically measured sand mining budget for the Mekong Delta reveals rising trends and significant volume underestimations. *Int. J. Appl. Earth Obs. Geoinf.* 108, 102736.

- Guan, B., Chen, M., Elsey-Quirk, T., Yang, S., Shang, W., Li, Y., Tian, X., Han, G., 2019. Soil seed bank and vegetation differences following channel diversion in the Yellow River Delta. *Sci. Total Environ.* 693, 133600.
- Gugliotta, M., Saito, Y., Nguyen, V.L., Ta, T.K.O., Nakashima, R., Tamura, T., Uehara, K., Katsuki, K., Yamamoto, S., 2017. Process regime, salinity, morphological, and sedimentary trends along the fluvial to marine transition zone of the mixed-energy Mekong River delta, Vietnam. *Cont. Shelf Res.* 147, 7–26.
- Ha, D.T., Ouilion, S., Vinh, G.V., 2018. Water and suspended sediment budgets in the lower Mekong from high-frequency measurements (2009–2016). *Water* 10, 846.
- Hackney, C.R., Darby, S.E., Parsons, D.R., Leyland, J., Best, J.L., Aalto, R., Nicholas, A.P., Houseago, R.C., 2020. River bank instability from unsustainable sand mining in the lower Mekong River. *Nat. Sustain.* 3, 217–225.
- Hecht, J.S., Lacombe, G., Arias, M.E., Dang, T.D., 2019. Hydropower dams of the Mekong River basin: a review of their hydrological impacts. *J. Hydrol.* 568, 285–300.
- Hein, H., Hein, B., Pohlmann, T., 2013. Recent sediment dynamics in the region of Mekong water influence. *Glob. Planet. Chang.* 110, 183–194.
- Hervouet, J.M., 2007. *Hydrodynamics of Free Surface Flows*. John Wiley and Sons, USA.
- Hung, N.N., Delgado, J.M., Güntner, A., Merz, B., Bárdossy, A., Apel, H., 2014a. Sedimentation in the floodplains of the Mekong Delta, Vietnam. Part I: suspended sediment dynamics. *Hydrol. Process.* 28, 3132–3144.
- Hung, N.N., Delgado, J.M., Güntner, A., Merz, B., Bárdossy, A., Apel, H., 2014b. Sedimentation in the floodplains of the Mekong Delta, Vietnam. Part II: deposition and erosion. *Hydrol. Process.* 28, 3145–3160.
- Jordan, C., Tiede, J., Lojek, O., Visscher, J., Apel, H., Nguyen, H.Q., Quang, C.N.X., Schlurmann, T., 2019. Sand mining in the Mekong Delta revisited – current scales of local sediment deficits. *Sci. Rep.* 9, 17823.
- Jordan, C., Visscher, J., Dung, N.V., Apel, H., Schlurmann, T., 2020. Impacts of human activity and global changes on future morphodynamics within the Tien River, Vietnamese Mekong Delta. *Water* 12 (8), 2204.
- Khoi, D.N., Dang, T.D., Pham, L.T.H., Loi, P.T., Thuy, N.T.D., Phung, N.K., Bay, N.T., 2020. Morphological change assessment from intertidal to river-dominated zones using multiple-satellite imagery: a case study of the Vietnamese Mekong Delta. *Reg. Stud. Mar. Sci.* 34, 101087.
- Koehnken, L., 2014. *Discharge Sediment Monitoring Project (DSMP) 2009–2013 Summary & Analysis of Results. Final Report. Mekong River Commission/ Gesellschaft für Internationale Zusammenarbeit, Phnom Penh, Cambodia.*
- Kondolf, G.M., Gao, Y., Annadale, G.W., Morris, G.L., Jiang, E., Zhang, J., Cao, Y., Carling, P., Fu, K., Guo, Q., Hotchkiss, R., Peteuil, C., Sumi, T., Wang, H.W., Wang, Z., Wei, Z., Wu, B., Wu, C., Yang, C.T., 2014a. Sustainable sediment management in reservoirs and regulated rivers: experiences from five continents. *Earth's Future* 2, 256–280.
- Kondolf, G.M., Rubin, Z.K., Minear, J.T., 2014b. Dams on the Mekong: cumulative sediment starvation. *Water Resour. Res.* 50, 5158–5169.
- Kummu, M., Varis, O., 2007. Sediment-related impacts due to upstream reservoir trapping, the lower Mekong River. *Geomorphology* 85, 275–293.
- Kummu, M., Lu, X.X., Wang, J.J., Varis, O., 2010. Basin-wide sediment trapping efficiency of emerging reservoirs along the Mekong. *Geomorphology* 119, 181–197.
- Langendoen, E.J., Mendoza, A., Abad, J.D., Tassi, P., Wang, D., Ata, R., El kadi Abderrezzak, K., Hervouet, J.M., 2016. Improved numerical modelling of morphodynamics of rivers with steep banks. *Adv. Water Res.* 93, 4–14.
- Lauri, H., De-Moel, H., Ward, P.J., Räsänen, T.A., Keskinen, M., Kummu, M., 2012. Future changes in Mekong River hydrology: impact of climate change and reservoir operation on discharge. *Hydrol. Earth Syst. Sci.* 16 (12), 4603–4619.
- Le, H.A., 2020. *Field And Model Investigation of Flow And Sediment Transport in the Lower Mekong River. Doctoral dissertation. Louvain-la-Neuve*, 151 pp.
- Lepesqueur, J., Hostache, R., Martínez-Carreras, N., Montargès-Pelletier, E., Hissler, C., 2019. Sediment transport modelling in riverine environments: on the importance of grain-size distribution, sediment density and boundary conditions. *Hydrol. Earth Syst. Sci.* 23, 3901–3915.
- Letrong, T., Li, Q., Li, Y., Vukien, T., Nguyenhai, Q., 2013. Morphology evolution of Cuadaí estuary, Mekong River, southern Vietnam. *J. Hydraul. Eng.* 18, 1122–1132.
- Li, X., Liu, J.P., Saito, Y., Nguyen, V.L., 2017. Recent evolution of the Mekong Delta and the impacts of dams. *Earth Sci. Rev.* 175, 1–17.
- Loc, H.H., Binh, D.V., Park, E., Shrestha, S., Dung, T.D., Son, V.H., Truc, N.H.T., Mai, N. P., Seijger, C., 2021. Intensifying saline water intrusion and drought in the Mekong Delta: from physical evidence to policy outlooks. *Sci. Total Environ.* 757, 143919.
- Loisel, H., Mangin, A., Vantrepotte, V., Dessailly, D., Dinh, D.N., Garnesson, P., Ouilion, S., Lefebvre, X.P., Meriaux, X., Phan, T.M., 2014. Remote sensing of environment variability of suspended particulate matter concentration in coastal waters under the Mekong's influence from ocean color (MERIS) remote sensing over the last decade. *Remote Sens. Environ.* 150, 218–230.
- Lu, X.X., Siew, R.Y., 2006. Water discharge and sediment flux changes over the past decades in the lower Mekong River: possible impacts of the Chinese dams. *Hydrol. Earth Syst. Sci.* 10, 181–195.
- Lu, X.X., Li, S., Kummu, M., Padawangi, R., Wang, J.J., 2014. Observed changes in the water flow at Chiang Saen in the lower Mekong: impacts of Chinese dams? *Quat. Int.* 336, 145–157.
- Lu, X.X., Oeurmg, C., Le, T.P.Q., Thuy, D.T., 2015. Sediment budget as affected by construction of a sequence of dams in the lower Red River, Vietnam. *Geomorphology* 248, 125–133.
- Mai, N.P., Kantoush, S., Sumi, T., Thang, T.D., Trung, L.V., Binh, D.V., 2018. Assessing and adapting the impacts of dams operation and sea level rising on saltwater intrusion into the Vietnamese Mekong Delta. *J. Jpn. Soc. Civ. Eng. Ser. B1 (Hydraul. Eng.)* 74, 373–378.
- Mai, N.P., Kantoush, S., Sumi, T., Thang, T.D., Binh, D.V., Trung, L.V., 2019. The influences of tidal regime and morphology change on salinity intrusion in Hau River. In: *E-proceedings of the 38th IAHR World Congress, Panama City, Panama.*
- Mai, N.P., Kantoush, S., Sumi, T., Thang, T.D., Binh, D.V., Trung, L.V., 2019b. Study on salinity intrusion processes into Hau River of Vietnamese Mekong Delta. *J. Jpn. Soc. Civ. Eng. Ser. B1 (Hydraul. Eng.)* 75 (2), 751–756.
- Manh, N.V., Dung, N.V., Hung, N.N., Kummu, M., Merz, B., Apel, H., 2015. Future sediment dynamics in the Mekong Delta floodplains: impacts of hydropower development, climate change and sea level rise. *Glob. Planet. Chang.* 127, 22–33.
- Manh, N.V., Dung, N.V., Hung, N.N., Merz, B., Apel, H., 2014. Large-scale suspended sediment transport and sediment deposition in the Mekong Delta. *Hydrol. Earth Syst. Sci.* 18, 3033–3053.
- Maeda, E.E., Formaggio, A.R., Shimabukuro, Y.E., 2008. Impacts of land use and land cover changes on sediment yield in a Brazilian Amazon drainage basin. *GI Sci. Remote Sens.* 45 (4), 443–453.
- Milliman, J.D., Farnsworth, K.L., 2011. *River Discharge to the Coastal Ocean: A Global Synthesis*. Cambridge University Press.
- Minderhoud, P.S.J., Middelkoop, H., Erkens, G., Stouthamer, E., 2020. Groundwater extraction may drown mega-delta: projections of extraction-induced subsidence and elevation of the Mekong delta for the 21st century. *Environ. Res. Commun.* 2, 011005.
- Mtamba, J., Velde, T.V.D., Ndomba, P., Zoltán, V., Mitalo, F., 2015. Use of radarsat-2 and Landsat TM images for spatial parameterization of Manning's roughness coefficient in hydraulic modeling. *Remote Sens.* 7, 836–864.
- Nowacki, D.J., Ogston, A.S., Nittrouer, C.A., Fricke, A.T., Van, P.D.T., 2015. Sediment dynamics in the lower Mekong River: transition from tidal river to estuary. *J. Geophys. Res. Oceans* 120, 6363–6383.
- Sisyph, 2018. *Sisyph User Manual, Version v7p3*, 70 pp.
- Pahl, J.W., Freeman, A.M., Raynie, R.C., Day, J., 2020. Response of the coastal systems to freshwater input with emphasis on Mississippi River deltaic plain river diversions: Synthesis of the state of the science. *Estuar. Coast. Shelf Sci.* 243, 106866.
- Park, E., Ho, H.L., Tran, D.D., Yang, X., Alcantara, E., Merino, E., Son, V.H., 2020. Dramatic decrease of flood frequency in the Mekong Delta due to river-bed mining and dyke construction. *Sci. Total Environ.* 723, 138066.
- Park, E., Ho, H.L., Binh, D.V., Kantoush, S., Poh, D., Alcantara, E., Try, S., Lin, Y.N., 2022. Impacts of agricultural expansion on floodplain water and sediment budgets in the Mekong River. *J. Hydrol.* 605, 127296.
- Rice, S.P., Roy, A.G., Rhoads, B.L., 2008. *River Confluences, Tributaries And the Fluvial Network*. John Wiley, Chichester, UK.
- Schmitt, R.J.P., Giuliani, M., Bizzi, S., Kondolf, G.M., Daily, G.C., Castelletti, A., 2021. Strategic basin and delta planning increases the resilience of the Mekong Delta under future uncertainty. *PNAS* 118 (36), e2026127118.
- Stokes, G., 1851. *On the Effect of the Internal Friction of Fluids on the Motion of Pendulums*. Cambridge Pitt Press, Cambridge.
- Thanh, V.Q., Reynolds, J., Wackerman, C., Eidam, E.F., Roelvink, D., 2017. Modelling suspended sediment dynamics on the subaqueous delta of the Mekong River. *Cont. Shelf Res.* 147, 213–230.
- Thuy, N.T.D., Khoi, D.N., Nhan, D.T., Nga, T.N.Q., Bay, N.T., Phung, N.K., 2019. Modelling accretion and erosion processes in the Bassac and Mekong Rivers of the Vietnamese Mekong Delta. In: Viet, N.T., Xiping, D., Tung, T.T. (Eds.), *Proceeding of the 10th International Conference on Asian and Pacific Coasts*, 2019, Hanoi, Vietnam. Springer, Hanoi, pp. 1431–1437.
- Tran, D.A., Tsujimura, M., Pham, H.V., Nguyen, T.V., Ho, L.H., Vo, P.L., Ha, K.Q., Dang, T.D., Binh, D.V., Doan, Q.V., 2021. Intensified salinity intrusion in coastal aquifers due to groundwater overextraction: a case study in the Mekong Delta, Vietnam. *Environ. Sci. Pollut. Res.* 29, 8996–9010.
- Tu, L.X., Thanh, V.Q., Reynolds, J., Van, S.P., Anh, D.T., Dang, T.D., Roelvink, D., 2019. Sediment transport and morphodynamical modeling on the estuaries and coastal zone of the Vietnamese Mekong Delta. *Cont. Shelf Res.* 186, 64–76.
- Van, P.D.T., Popescu, I., Van Griensven, A., Solomatine, D.P., Trung, N.H., Green, A., 2012. A study of the climate change impacts on fluvial flood propagation in the Vietnamese Mekong Delta. *Hydrol. Earth Syst. Sci.* 16, 4637–4649.
- Villaret, C., Hervouet, J.M., Kopmann, R., Merkel, U., Davies, A.G., 2013. Morphodynamic modelling using the Telemac finite element system. *Comput. Geosci.* 53 (105–113), 2013.
- Vinh, V.D., Ouilion, S., Van Thao, N., Ngoc Tien, N., 2016. Numerical simulations of suspended sediment dynamics due to seasonal forcing in the Mekong coastal area. *Water* 8, 255.
- Wassmann, R., Hien, N.X., Hoanh, C.T., Tuong, T.P., 2004. Sea level rise affecting the Vietnamese Mekong Delta: water elevation in the flood season and implications for rice production. *Clim. Chang.* 66, 89–107.
- Wolanski, E., Huan, N.N., Dao, L.T., Nhan, N.H., Thuy, N.N., 1996. Fine-sediment dynamics in the Mekong River Estuary, Viet Nam. *Estuar. Coast. Shelf Sci.* 43, 565–582.
- Xing, F., Meselhe, E.A., Allison, M.A., Weathers III, H.D., 2017. Analysis and numerical modeling of the flow and sand dynamics in the lower Song Hau channel, Mekong Delta. *Cont. Shelf Res.* 147, 62–77.
- Xue, Z., He, R., Liu, J.P., Warner, J.C., 2012. Modeling transport and deposition of the Mekong River sediment. *Cont. Shelf Res.* 37, 66–78.